

Supplementary information for

A thermosensitive hydrogel achieves sustained co-delivery of two therapeutic agents with distinct properties for preventing aseptic loosening

Yang Wang^a, Xin Wang^a, Hongjie Zhang^a, Yaoben Wang^a, Hancheng Wang^a, Zhiyong Chen^a,
Jiandong Ding^a, Xiaochun Peng^{b,*}, Lin Yu^{a,c,*}

^aState Key Laboratory of Molecular Engineering of Polymers, Department of Macromolecular
Science, Shanghai Stomatological Hospital and School of Stomatology, Fudan University,
Shanghai 200438, P. R. China

^bDepartment of Orthopedics, Shanghai Sixth People's Hospital Affiliated to Shanghai Jiao Tong
University School of Medicine, Shanghai 200233, P. R. China

^cShanghai Key Laboratory of Gene Editing and Cell Therapy for Rare Diseases, Fudan University,
Shanghai 200031, P. R. China

*Corresponding authors. E-mail: yu_lin@fudan.edu.cn (L. Yu) and dr.xcpeng@shsmu.edu.cn
(X.C. Peng)

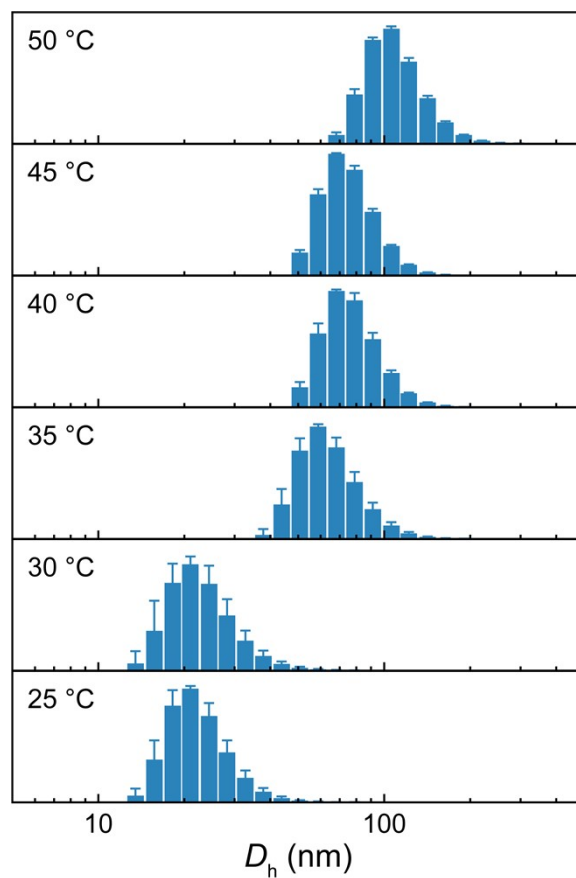


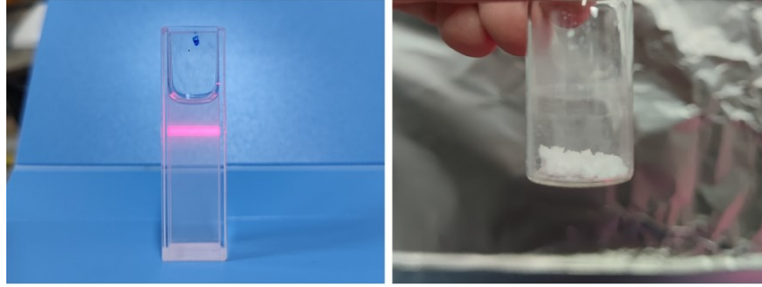
Fig. S1 Size and distribution of copolymer micelles formed in a 1 wt% PLGA-PEG-PLGA aqueous solution at different temperatures. The average D_h increased from 22.8 nm to 111.1 nm upon heating.



Mixture solution

Mixture of
drugs and polymers

Fig. S2 Optical images of the two-step method. The homogeneous solution of Emo and PLGA-PEG-PLGA copolymers in the mixed solvent of ethanol and acetonitrile is shown on the left, while the uniform yellow Emo-copolymer mixture adhered to the flask wall after rotary evaporation is presented on the right.



The suspension
after desolvation

Lyophilized sCT/BSA NPs

Fig. S3 Optical images of the desolvation method. The suspension of sCT/BSA NPs after ethanol-induced desolvation exhibits the Tyndall effect (left), and the lyophilized powder of sCT/BSA NPs is shown on the right.

Table S1 Surface charge density of sCT/BSA NPs at different weight ratios, BSA NPs and free sCT in water

sCT/BSA weight ratio	W_{sCT} ^a	ζ (mV) ^b	σ (C·m ⁻²) ^c
0.0625	0.059	-60.23	-5.41×10^{-5}
0.125	0.111	-59.47	-5.32×10^{-5}
0.25	0.200	-47.83	-3.97×10^{-5}
0.5	0.333	-44.47	-3.62×10^{-5}
1	0.500	-37.47	-2.95×10^{-5}
2	0.667	-18.73	-1.38×10^{-5}
4	0.800	-0.17	-0.01×10^{-5}
8	0.889	26.50	2.00×10^{-5}
16	0.941	27.37	2.07×10^{-5}
BSA NPs	\	-71.27	-6.96×10^{-5}
Free sCT	\	27.43	2.08×10^{-5}

^a Calculated from the corresponding sCT/BSA weight ratio;

^b Obtained from Figure 4C;

^c Calculated via equation (1), and the parameter values used in equation (1) are as follows: the Avogadro constant (N_A) = 6.022×10^{23} mol⁻¹, the Boltzmann constant (k_B) = 1.381×10^{-23} J·K⁻¹, the elementary charge (e) = 1.602×10^{-19} C, temperature (T) = 298.15 K, the vacuum permittivity (ϵ_0) = 8.854×10^{-12} F·m⁻¹ and the relative permittivity of water in 298.15 K ($\epsilon_{r, \text{water}}$) = 78.4.

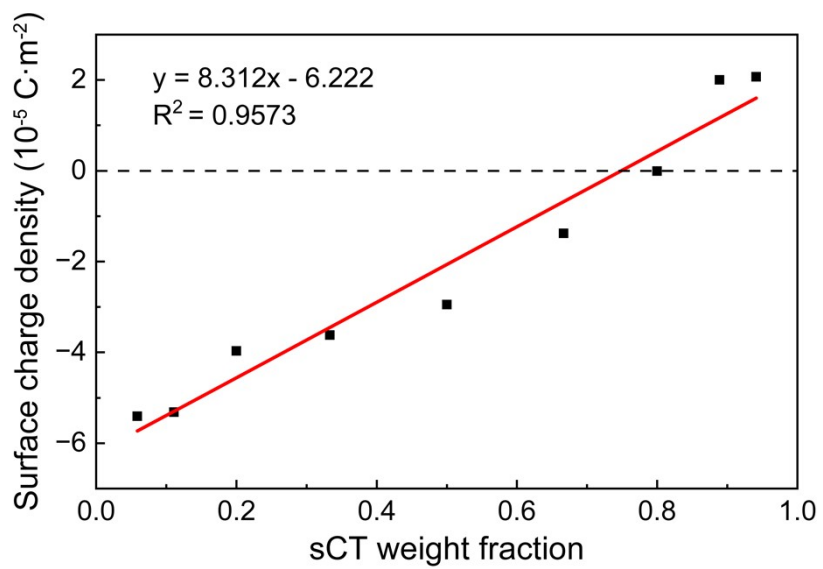


Fig. S4 Surface charge density of sCT/BSA NPs as a function of sCT weight fraction in NPs. The slope of the fitted curve is 8.312 ± 0.663 , and the intercept is -6.222 ± 0.394 .

Table S2 Specific gravity analysis of secondary structure of free sCT and sCT/BSA NPs at the weight ratio of 4

	Free sCT	Free sCT at pH 10	sCT/BSA NPs
α -Helix	11.1%	11.1%	11.2%
β -Turn	23.2%	23.2%	23.2%
Random coil	55.8%	55.8%	55.7%
Parallel	19.0%	19.0%	19.0%
Anti-parallel	21.0%	21.0%	20.9%

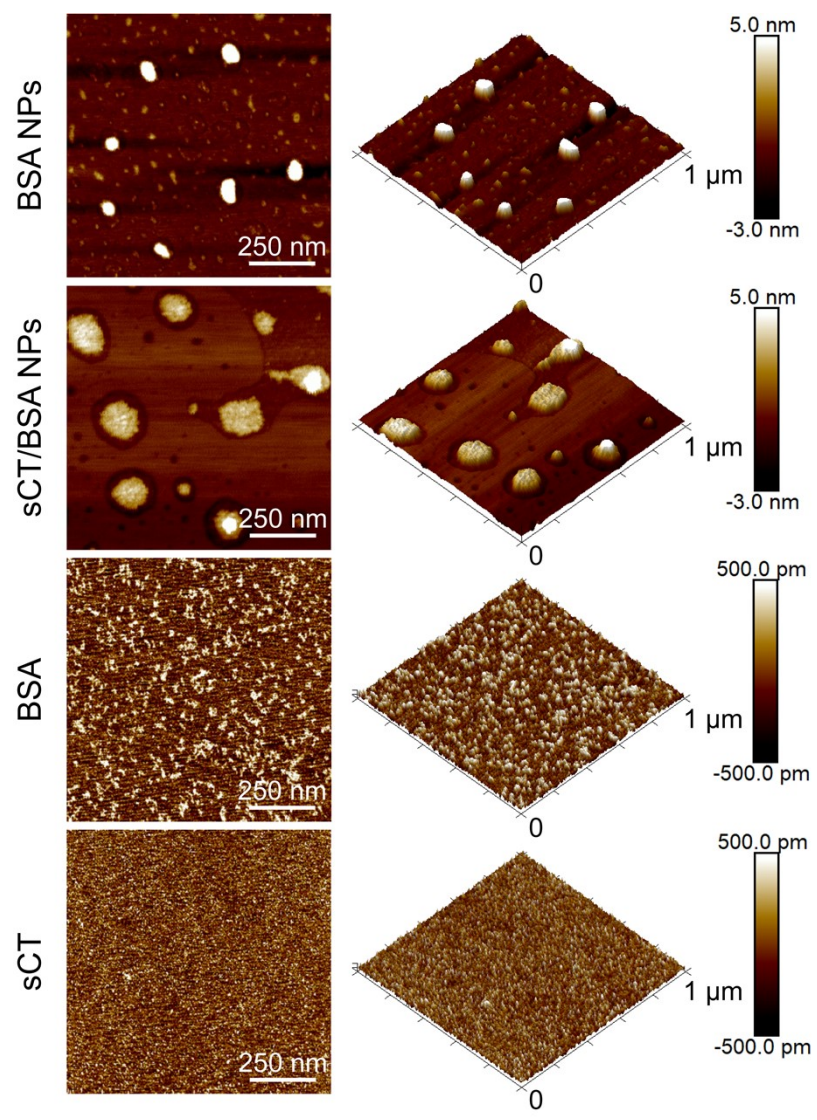


Fig. S5 AFM images of BSA NPs, sCT/BSA NPs, free BSA and free sCT.

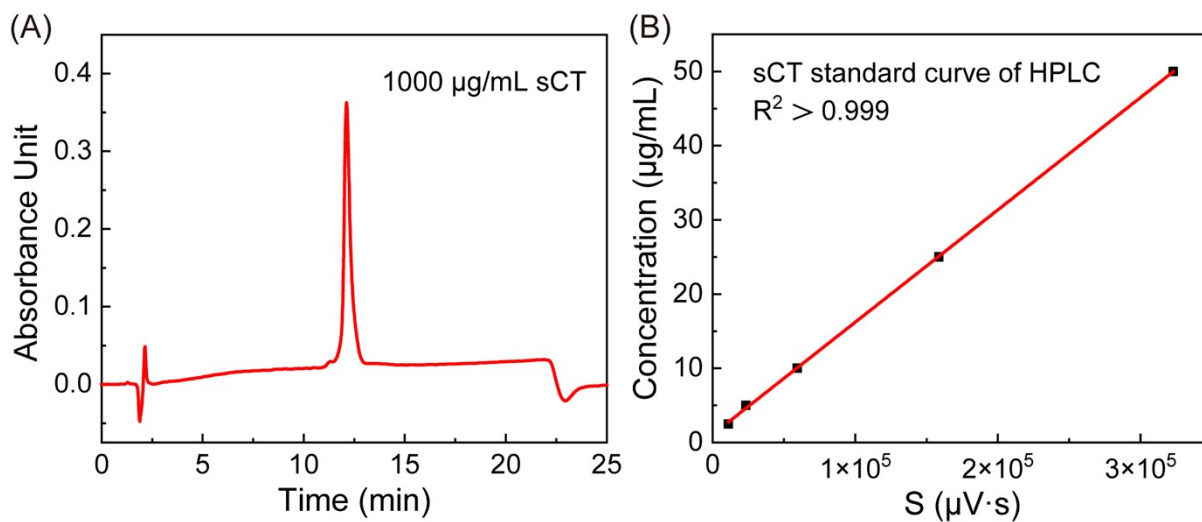


Fig. S6 (A) HPLC elution curve of sCT detected at 220 nm. (B) Standard curve of sCT established by HPLC. The linear fitting resulted in $y = 0.00015x + 1.1$, $R^2 = 0.9998$.

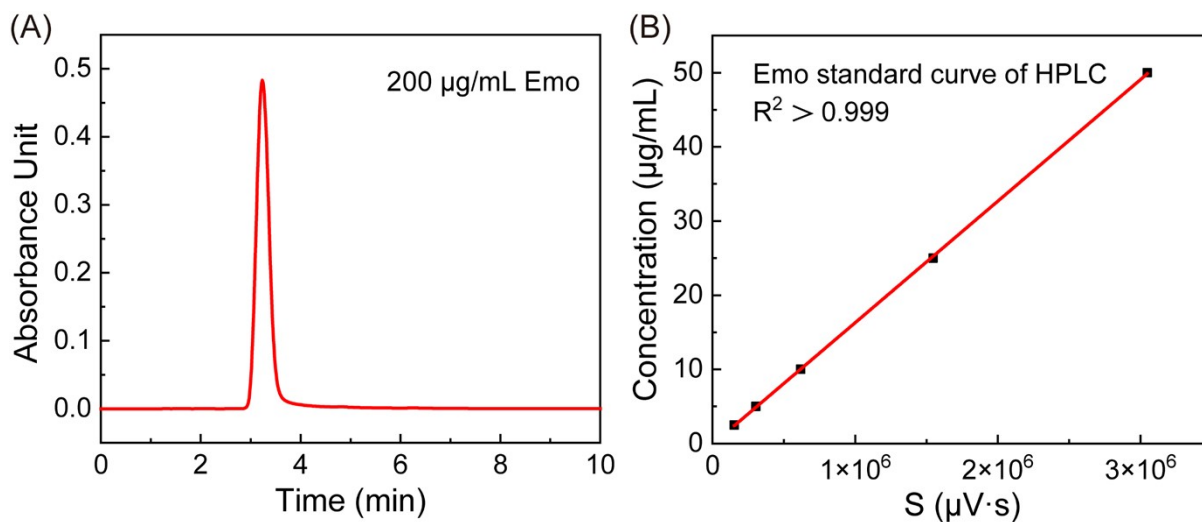


Fig. S7 (A) HPLC elution curve of Emo detected at 222 nm. (B) Standard curve of Emo established by HPLC. The linear fitting resulted in $y = 0.000016x - 0.094$, $R^2 = 0.9999$.

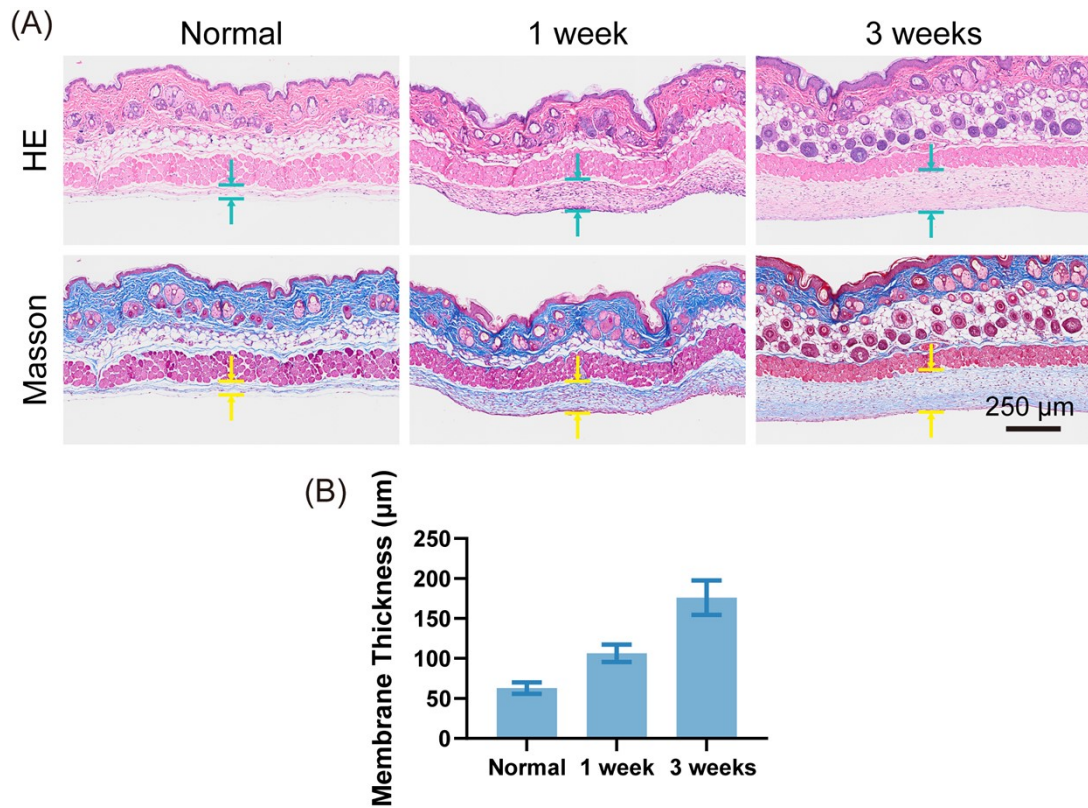


Fig. S8 (A) Histological section images of the pouch membrane stained with HE and Masson' s trichrome. Normal: dorsal skin from a normal mouse, 1 week: skin tissue from the air pouch maintained for one week, 3 weeks: skin tissue from the air pouch maintained for three weeks. Green and yellow arrows denote the pouch membranes. (B) Statistical analysis of the pouch membrane thickness. Error bars denote the SD of data ($n = 3$).

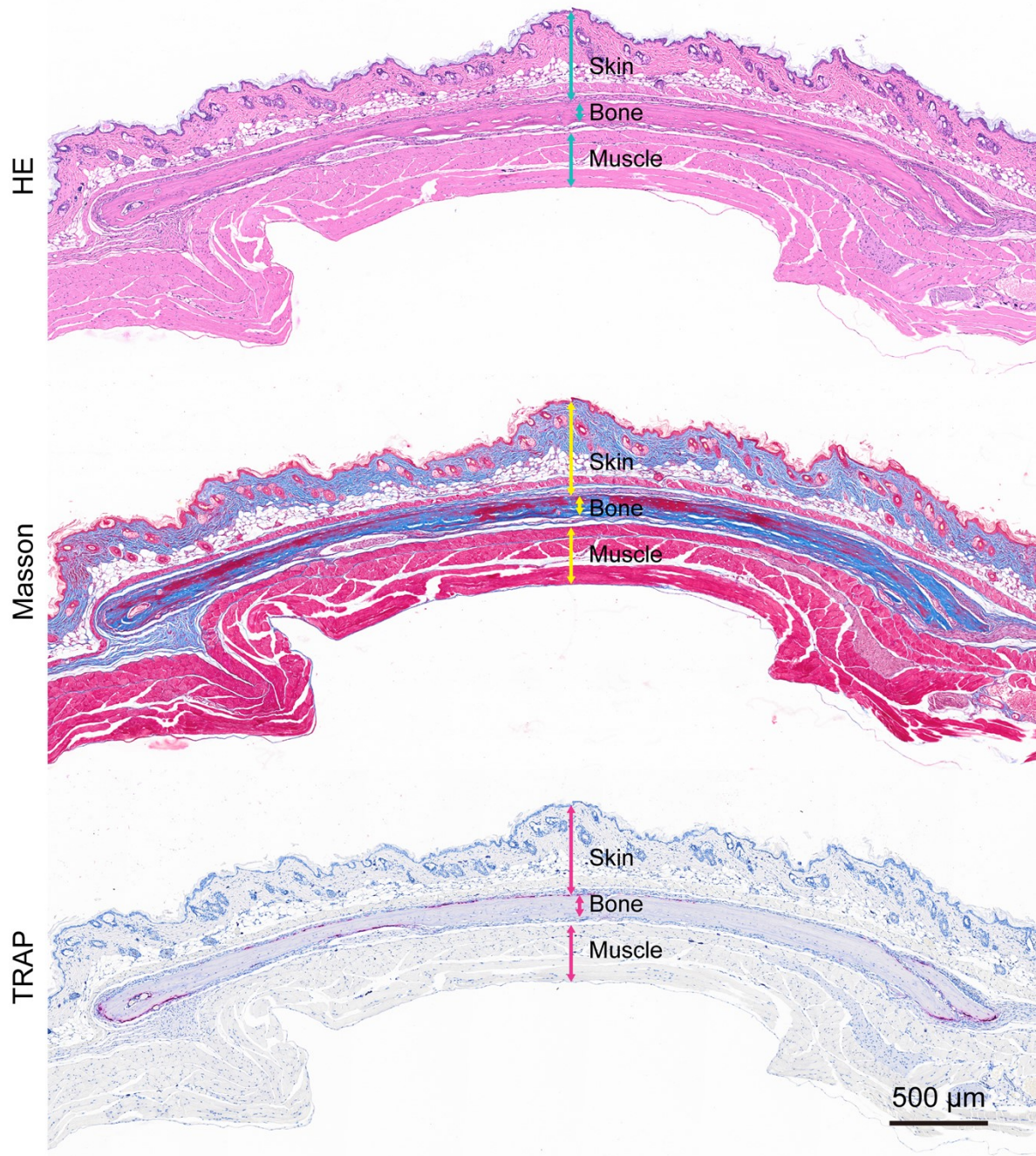


Fig. S9 Representative histological section images of bone-implanted pouch “sandwich”-like tissues from the Sham group stained with HE, Masson’s trichrome and TRAP.

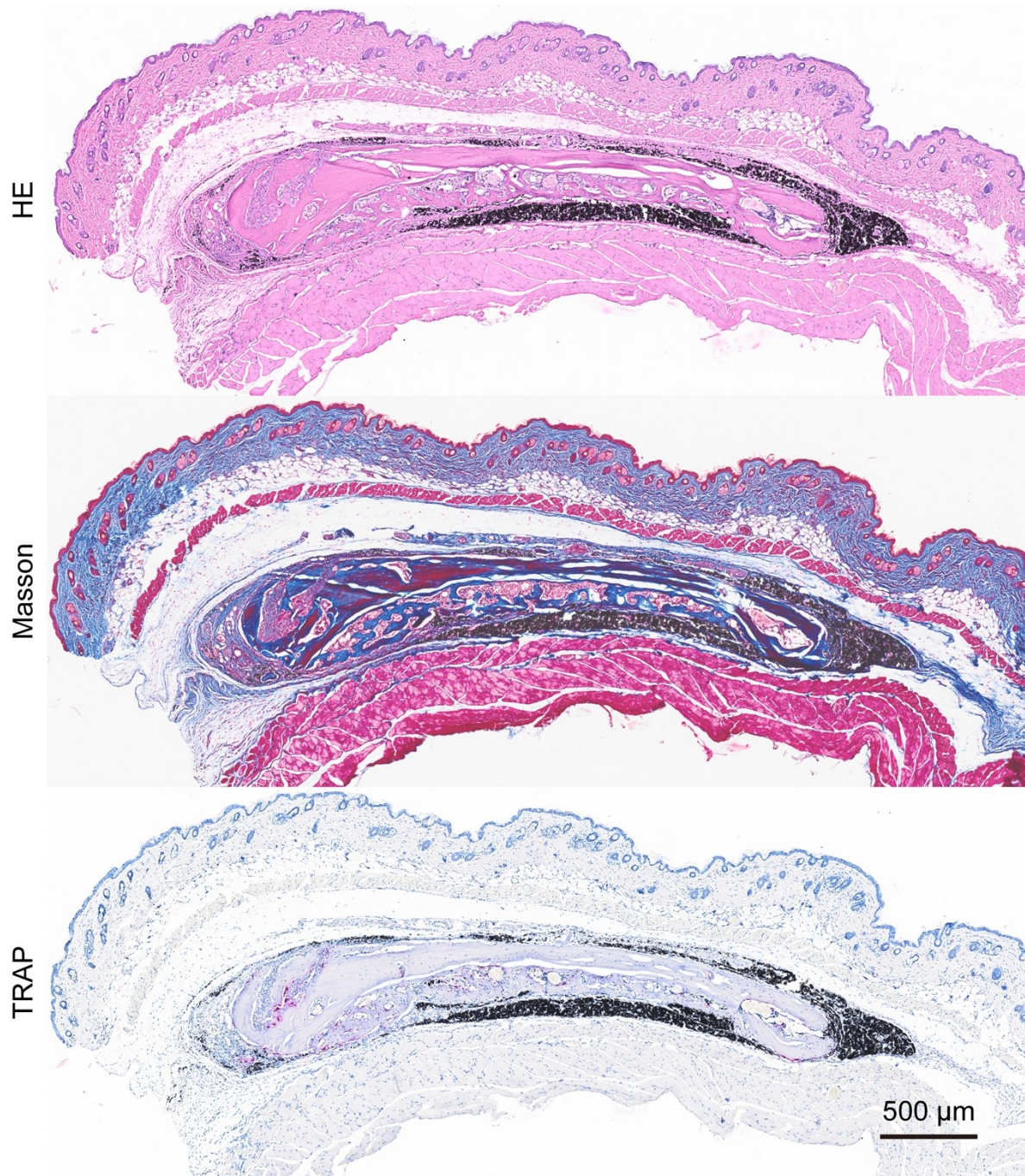


Fig. S10 Representative histological section images of bone-implanted pouch “sandwich”-like tissues from the Untreated group stained with HE, Masson’s trichrome and TRAP.